J. Membrane Biol. 175, 87–93 (2000)

The Journal of
Membrane
Biology

Effects of Na^+ on the Predominant K^+ Channel in the Tonoplast of *Chara:* Decrease of Conductance by Blocks in 100 Nanosecond Range and Induction of Oligo- or Poly-subconductance Gating Modes

R. Weise, D. Gradmann

Abteilung Biophysik der Pflanze, Albrecht-von-Haller-Institut für Pflanzenwissenschaften, Universität Göttingen, Untere Karspüle 2, D-37073 Göttingen, Germany

Received: 16 November 1999/Revised: 8 February 2000

Abstract. We present three mechanisms by which Na^+ inhibits the open channel currents of the predominant K^+ channel in the tonoplast of *Chara corallina:* (i) Fast block, i.e., short (100 *ns* range) interruptions of the open channel current which are determined by open channel noise analysis, (ii): Oligo-subconductance mode, i.e., a gating mode which occurs preferentially in the presence of Na^+; this mode comprises a discrete number (here 3) of open states with smaller conductances than normal, and (iii): Polysubconductance mode, i.e., a gating mode with a nondiscrete, large number (>30) of states with smaller conductances than the main open channel conductance. This novel mode has also been observed only in the presence of Na^+.

Key words: *Chara corallina* — Fast Na^+ block — Gating — Subconductance — Patch clamp — Open channel noise

Introduction

Open channel conductance is a key parameter for the function of ion channels. The 'conductance' of an open channel is mostly a crude Ohmic approach to a nonlinear current-voltage-relationship.

The exact shape of an open channel current-voltage relationship depends on many details, such as the presence of alternate non- or less-conducted ions which compete with the predominant transportee. Typically, these inhibitory effects increase with the electrochemical distance from equilibrium. For instance, in the predominant K^+ channel in the tonoplast of *Chara* ($Ch_{T,K}$), Na^+ causes the apparent open channel current-voltage relationship to tend towards zero current at both ends (Bertl, 1989). Such inhibitory effects of various cations (Na^+, Rb^+, Cs^+, and Ca^{2+}) have been investigated systematically, with particular emphasis on the effect of luminal Cs^+ on inward currents (in contrast to Na^+, luminal Cs^+ has no effect on the outward currents), which could be demonstrated statistically to consist of short, Cs^+-induced interruptions of normal K^+ currents (Klieber & Gradmann 1993). This mode is commonly called 'fast block', a term which does not express the characteristic cooperativity with the voltage distance from equilibrium. Draber and Hansen (1994) have confirmed this interpretation of the fast Cs^+ block by direct observations of fast switching with advanced techniques (Schultze & Draber, 1993). In this situation, it was a challenge to examine whether the other cases of cooperative inhibition of the apparent open-channel conductance by voltage and competing cations can also be resolved in terms of fast blocking. Here, we focused on the effect of cytoplasmic Na^+ on the outward conductance, because this effect is more pronounced than the inhibition of the inward conductance by luminal Na^+ (Bertl, 1989). Furthermore, inhibitory effects of cytoplasmic Na^+ on K^+ outward currents are expected to be physiologically relevant as under salt stress, when inward leaking Na^+ inhibits loss of cytoplasmic K^+.

So it was not surprising to find, in addition to fast Na^+ block, 'subconductance' modes of $Ch_{T,K}$-inhibition by cytoplasmic Na^+, i.e., infrequent open states with a smaller conductance than normal. In particular, we describe a novel, *polysubconductance* gating mode of $Ch_{T,K}$ which appeared only in the presence of Na^+. The second, major aim of this study is to present and to discuss this novel phenomenon in the context of a more familiar type of gating mode, an oligosubconductance

Correspondence to: D. Gradmann

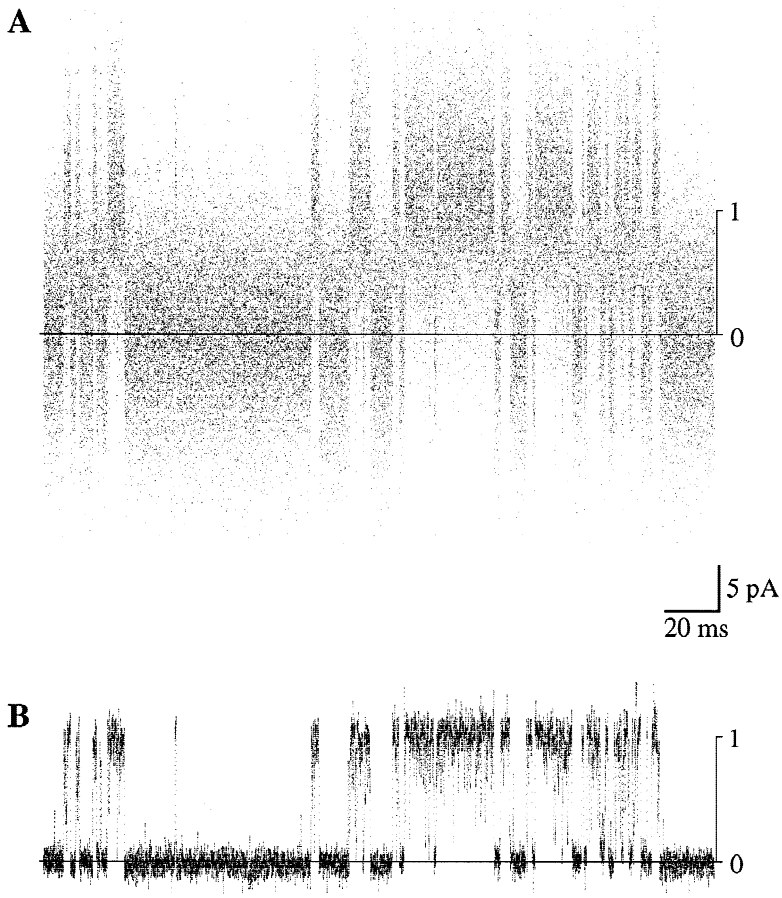

Fig. 1. Original recording of single channel currents under reference conditions: symmetric 150 mM KCl plus 1 mM $CaCl_2$, $V = 100$ mV; 0: baseline; 1: mean open current; (*A*) filtered with 50 kHz (4-pole Bessel); (*B*) same data as in *A* but filtered with 3 kHz (Gauss).

state of $Ch_{T,K}$ which was also observed in the presence of Na^+ here.

Materials and Methods

$Ch_{T,K}$ has been investigated by standard patch-clamp techniques according to Klieber and Gradmann (1993) with some modifications. For improvement of the seal between glass and membrane, the glass pipettes have treated: (i) internal coating with Sigmacote (Sigma Chemical) and subsequent drying over night before pulling, (ii) external coating with Sylgard (Dow Corning) and heat polishing after pulling according to Penner (1995). After this processing, the pipettes have been stored under glass no longer than 6 hr before use. The measuring chamber had a volume of about 10 μl and a perfusion device according to Lühring (1999). To reduce pipette noise during a recording, the measuring pipette with isolated patch was dipped as superficial as possible into the bath.

Time series of small currents have been recorded by a Dagan amplifier (Dagan, Model 3900A) with a 4-pole Bessel output filter. The analog data have been digitized by a 16 bit A/D converter (ITC 16, Instrutech Corp.) and transferred to a computer. If not noted otherwise, all signals have been lowpass filtered by 50 kHz (4-pole Bessel) and sampled with 200 kHz. Aliasing artifacts have been eliminated by using only the twelve most significant bits. In parallel, the output data have been lowpass filtered (8-pole Bessel) usually between 1 and 5 kHz and displayed on an oscilloscope for immediate observation.

Custom tailored software was used to eliminate some common numerical artifacts. In longer recordings, for instance, ill-defined gaps between smaller data portions (blocks) have been avoided by continuous transfer of the original digitized data to the 96 MB RAM of a personal computer (Macintosh PPC-604/150), and later transferred as an individual block to the hard disk. Furthermore, periodic irregularities in histograms are often due to binning artifacts. These artifacts have been avoided by binning of the original digitized data only in integer steps. Generation of selective amplitude histograms according to Patlak (1988) and application of advanced level detection (Schultze & Draber 1993) were also part of the software. The software for acquisition and analysis of the data is available on request. This study follows the sign convention (Bertl et al. 1992) for voltages and currents in endomembranes. All solutions were adjusted to pH 7.5 with 5 mM Hepes/KOH.

Results and Discussion

Fast Block Determined by Analysis of Open Channel Noise

An example of single-channel current recording from $Ch_{T,K}$ is shown in Fig. 1. Figure 1*A* illustrates the primary data as measured with maximum bandwidth. In

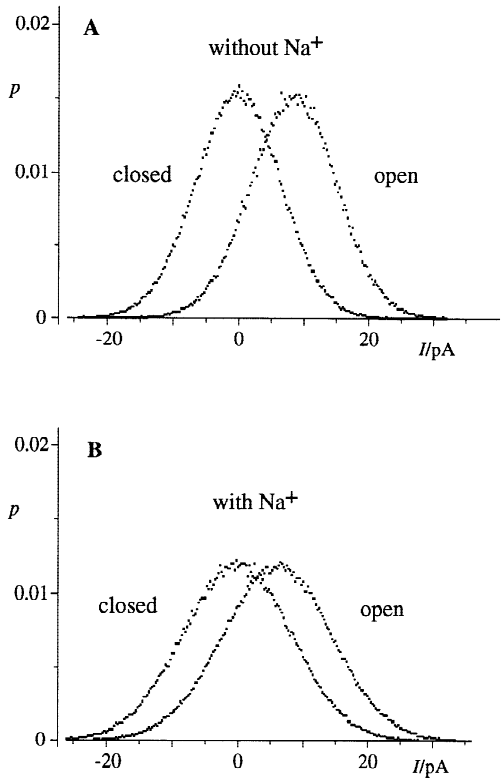

Fig. 2. Effect of Na^+ on amplitude and noise of open channel currents; conditions: cytoplasmic 0.1 mM Ca^{2+} and 250 mM K^+; luminal 1 mM Ca^{2+} and 150 mM K^+; sampling interval 5 μsec, filter: 50 kHz 4-pole Bessel; $V = 60$ mV; reference *A* without Na^+: baseline ($n = 2.6 \times 10^5$) 0 ± 6.54 pA, open channel current ($n = 1.1 \times 10^5$) −8.49 ± 6.63 pA; experiment (*B*) (same patch as in *A*) with additional 50 mM Na^+ on cytoplasmic side: baseline ($n = 2.1 \times 10^5$) 0 ± 8.33 pA, open channel current ($n = 3.0 \times 10^5$) −6.14 ± 8.42 pA; σ (= SD) determined for each current level separately after assignment of data series' to current levels by Hinkley detection with a temporal resolution of 50 μsec, according to Draber and Schultze (1993).

Fig. 1*B* and the subsequent illustrations of original traces the data have been low-pass filtered (digital Gaussian), simply to provide a more clear impression. However, the better appeal of filtered traces is traded in for loss of information or even introduction of pseudo-information: Compared to the baseline, the open channel current in Fig. 1*B* looks more noisy, and the additional noise seems to be asymmetrical, i.e., wider towards the baseline. In contrast, the amplitude histograms of the high frequency (≤50 kHz) data in Fig. 2*A* do not show much noise difference between the baseline and the channel current, neither in amount nor in shape. Only a detailed analysis by fitting Gaussian probability density functions to the experimental data reveals a slightly wider σ_o of the open channel recording ($\sigma_o = 6.63$ pA) compared to the baseline ($\sigma_b = 6.54$ pA). This would amount to an open channel noise of $\sigma_{ch} = (\sigma_o^2 - \sigma_b^2)^{0.5}$ of 1.09 pA.

In the equivalent experiment with the same patch after addition of 50 mM Na^+ to the cytoplasmic compartment (Fig. 2*B*), the mean open current (6.14 pA) is reduced to $\eta = 0.72$ of the open channel current in absence of Na^+ (8.49 pA). These results confirm the report of Bertl (1989). Noise analysis of these data yield $\sigma_{ch,Na} = (\sigma_{o,Na}^2 - \sigma_{b,Na}^2)^{0.5} \approx 1.16$ pA with $\sigma_{o,Na} = 8.41$ and $\sigma_{b,Na} = 8.33$ pA in the presence of Na^+ (the finding $\sigma_{b,Na} > \sigma_b$ was consistent throughout the experiments but no subject of further investigation here).

If the observation $\sigma_{ch,Na} > \sigma_{ch}$ were due to fast blockage the following analysis would apply according to FitzHugh (1983). We assume a channel which alternates between an open state with the mean life time τ_o, and a blocked state with the mean life time τ_b. At a given voltage, the current is 1 in the open state and 0 in the blocked state. The time course of the current is low-pass filtered with the time constant τ. The observed currents will follow a β-distribution of the form

$$y(x) = \chi^{a-1} \cdot (1 - x)^{b-1}, \tag{1}$$

with $a = \tau/\tau_o$, $b = \tau/\tau_b$, and the observed currents x ($0 < x < 1$). Numerical calculations show that for $\tau \gg \tau_o$ and τ_b, the β-distribution approaches a Gaussian distribution around $\eta = 1/(1 + \tau_b/\tau_o)$ with a σ proportional to the square root of the geometric mean of $1/a$ and $1/b$

$$\sigma = A \cdot \left(\frac{\tau_o \cdot \tau_b}{\tau^2} \right)^{1/4}, \tag{2}$$

where $A = 2^{-1.5} \approx 0.35$ is an empirical factor. If we substitute τ_b in Eq. (2) by $\tau_o \cdot (1 - \eta)/\eta$, τ_o can be isolated from this equation with the apparative parameter τ plus the observed parameters σ and η

$$\tau_o \approx 8\tau\sigma^2(\eta/(1 - \eta))^{0.5}. \tag{2a}$$

In our case for Na^+-induced widening of open channel noise $\sigma_{Na} = (\sigma_{ch,Na}^2 - \sigma_{ch}^2)^{0.5} \approx 0.40$ pA (measured: $\sigma_{ch,Na} = 1.16$, $\sigma_{ch} = 1.09$ pA), this σ_{Na} can be normalized to $\sigma = \sigma_{Na}/(8.49\text{ pA}) \approx 0.05$ with respect to the open channel current (8.49 pA) in the absence of Na^+. Furthermore, $\eta = 0.72$ is known from the experiments and $\tau = 4.5$ μsec from the empirical $\tau = 0.224/f_B$ (Klieber & Gradmann 1993) with the cutoff frequency $f_B = 50$ kHz of an 8-pole Bessel filter. With these numbers, Eq. (2*a*) yields the mean life time of the open state $\tau_o \approx 144$ nsec, and the mean duration of the Na^+-induced blockage, $\tau_b = \tau_o \cdot (1 - \eta)\eta$, is about 56 nsec. Independent recordings on five patches yielded similar results (mean $\tau_o \approx 300$ nsec, mean $\tau_b \approx 100$ nsec, SD ≈ 100%). The available data are, however, not sufficient to assess the sensitivity of τ_o and τ_b to V and the Na^+ concentration.

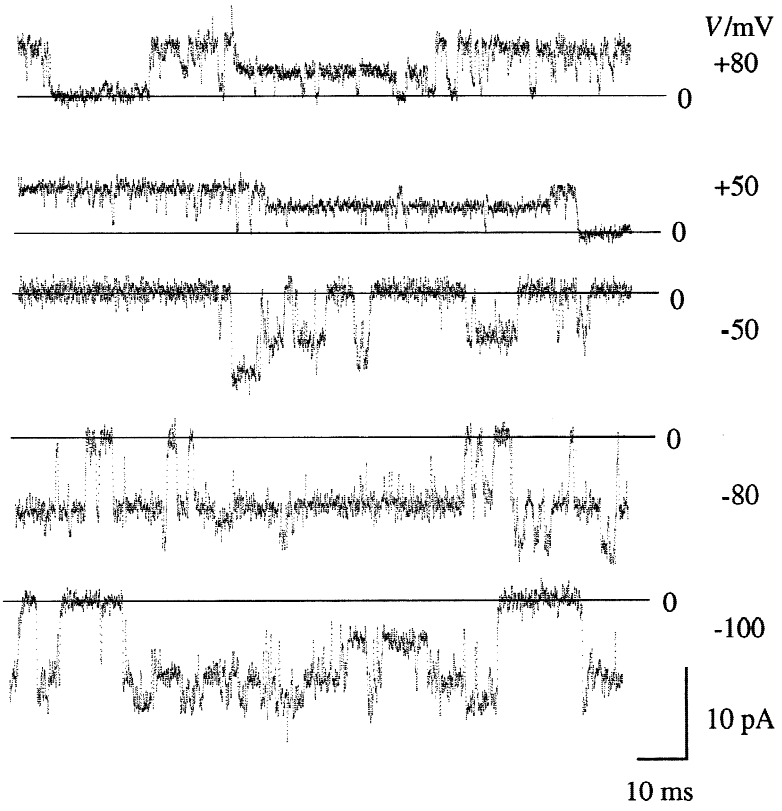

Fig. 3. Single channel current recordings in oligoconductance state at various voltages as indicated; 0: baseline; conditions: cytoplasmic and luminal 250 mM K^+, 1 mM Ca^{2+} and 20 mM Na^+; original data filtered with 4 kHz (Gaussian) for illustration purpose.

Subconductance Gating Modes

Despite of many reports of well defined gating modes of $Ch_{T,K}$ (e.g., Laver & Walker, 1987, Tyerman et al., 1992, Klieber & Gradmann 1993, Potossin et al., 1993, Draber & Hansen 1994, Hansen et al., 1997, Laver & Gage 1997, Laver et al., 1997, Lühring, 1999) there is unspoken consensus about the enormous variety of (unpublished) gating modes which occur only sporadically. Here we add two well-documented examples of such gating modes which comprise the occurrence of subconductance states. These two gating modes have been observed only in the presence of Na^+, indicating that fast blockage, discussed in the previous chapter, may not be the only mechanism by which Na^+ can reduce the time averaged K^+ conductance of $Ch_{T,K}$.

Oligosubconductance Mode

Figure 3 shows sections of original current records with $Ch_{T,K}$ displaying five distinct levels of conductance: zero conductance, full conductance and three intermediate 'sub'-conductances. From superficial inspection of Fig. 3 one might assume that these recordings are due to several channels. However, a more detailed analysis of the distribution of the current values (Fig. 4) shows that the current levels are not equidistant which would be

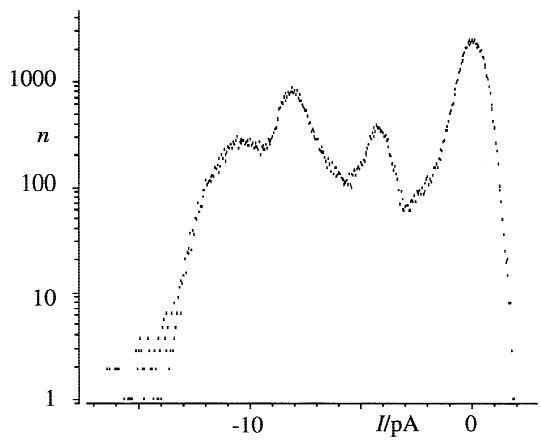

Fig. 4. Nonequidistant current-data accumulations during a time series ($V = -100$ mV) from experiment Fig. 3; selective amplitude histogram according to Patlak (1988) with exclusion criterium 2.5 pA (= SD of background noise), 200 μsec time window, and 20 kHz effective filtering.

expected if four channels of the same unitary conductance were responsible for the distribution. Also four channels with different unitary conductances could not produce the observed amplitude histogram (Fig. 4) because all the combinations from independently switching, heteroconducting channels would lead to many more (16) levels. A complete analysis of the kinetics of this

Table. Matrix of transitions between the conductance states 0 to 4

n_{ij}	0	1	2	3	4	p/%	i/pA	t/ms
0	—	**147**	**81**	**21**	**2**	**50**	**0**	**6.9**
	—	*72*	*51*	*21*	*3*	*50*	*0*	*11.9*
1	**202**	—	**375**	**38**	**5**	**15**	**−4.6**	**0.8**
	77	—	*121*	*15*	*2*	*15*	*−4.6*	*2.4*
2	**39**	**405**	—	**496**	**30**	**22**	**−8.2**	**0.8**
	45	*126*	—	*135*	*5*	*22*	*−8.2*	*2.4*
3	**6**	**61**	**494**	—	**197**	**9**	**−10.4**	**0.4**
	22	*15*	*133*	—	*36*	*9*	*−10.4*	*1.5*
4	**0**	**7**	**25**	**202**	—	**3**	**13.6**	**0.5**
	2	*3*	*5*	*36*	—	*3*	*−13.6*	*2.3*

Numbers of identified transitions from state i indexed in left column to state j indexed in top row; experiment Fig. 3; $V = -100$ mV, data volume: 3.5×10^5 data points in 1.75 sec; temporal resolution 80 μsec, (italics: *300* μsec); necessary correction for false alarms due to 1.4 pA background noise at 80 μsec resolution only for elements n_{23} and n_{32}: −7 and −3 events respectively; *p:* mean probability *i:* mean current at −100 mV, *t:* mean life time.

oligosubconductance gating mode is given by the transition matrix in the Table. This table shows that transitions between neighboring conductance states are most frequent but that there are also significant numbers of transitions to more distant states. So the reaction scheme for the five observed conductance levels consist of the linear 'backbone' 0-1-2-3-4 with infrequent transitions between nonneighboring states. One may visualize this by assuming that for, lets say the transition from 0 to 1, the (thermic) energy in state 0 happens to be large enough to surmount the energy barrier between state 0 and state 1; and that in rare cases, this energy is so high that state 2 can be reached in one step without an intermediate rest in state 1. The n_{ij} values in the Table can simply be converted to the rate constants

$$k_{ij} = (n_{ij}/p_i)/t \tag{3}$$

for the individual transitions from i to j, where p_i is the probability that the channel is found in state i and t is the total observation time. In principle, the n_{ij} values increase with better temporal resolution because more events could be detected on the short duration side. This is also reflected by the mean durations t which are divided in shorter fragments, as brief interruptions are detected. Only for the rare transitions from states >1 to state 0, more events have been counted at lower temporal resolution. These excess observations are due to nonresolved rests in intermediate states. Nevertheless, there are significant numbers of transitions between nonadjacent states.

So the seemingly confusion gating mode found in Fig. 3 is represented by the Table clearly, completely (with respect to the finite number of data) and fundamentally, i.e., in terms of microscopic transition probabilities k, which correspond to macroscopic rate constants of individual reaction steps.

Polysubconductance Mode

The current traces in Fig. 5 show $Ch_{T,K}$ in a gating mode with numerous subconductances at all voltages. The selective amplitude histogram (Fig. 6) of the recording at −120 mV shows a broad intermediate maximum between the sharp peaks of the baseline and the open channel level of about −18 pA. A more detailed analysis shows, however, that the intermediate maximum in Fig. 6 results from the superposition of many events with different conductances. These events have been identified individually as current stretches I_s of a detection time $t_d \geq 180$ μsec (i.e. ≥ 36 data points, or 1.6 times the rise time $t_{10-90} = 110$ μsec between 10 and 90% of a step response) which show not more scatter than the baseline. So the identified stretches marked current levels I_s of $t_s = t_d + t_{10-90} \geq 290$ μsec duration.

In Fig. 7, these durations, t_s, are plotted *vs.* the corresponding current amplitudes, I_s, for all the identified events of intermediate conductance. The current amplitudes are not clustered around a few predominant levels but are almost evenly distributed over the entire range with a certain accumulation around −11 pA. This accumulation corresponds to the broad, intermediate maximum in Fig. 6. A correlation between duration and amplitude of the isolated levels cannot be found in Fig. 7.

Thus, we may assume that for infinite observation times, this polyconductance mode will approach a *continuous* distribution of well confined current amplitudes, whereas in the oligoconductance mode the channel will assume only a few *discrete* amplitude levels.

For further analysis, these subconductance events have been sorted into three classes: S_1: subconductance events which started with a transition from the baseline and ended with a transition back to the baseline, S_3: subconductance events which started with a transition from the full conductance and ended with a transition back to the full conductance, and subconductances S_2 with other transitions. The ratios of the frequency of the three classes S_1:S_2:S_3 were approximately 2:3:5. Altogether, the channel spent about 8% of the total open time in a subconductance state. The amplitude histograms of these three classes (Fig. 8) differ slightly: S_1 has the most negative average current level, S_2 the most even distribution, and S_3 the sharpest peak. S_3 may correspond to the 'midstate' in a $Ch_{T,K}$ oligosubconductance mode which has been reported to alternate frequently with the full conductance state (Tyerman et al., 1992). The similarities (e.g., this preference of transitions) and

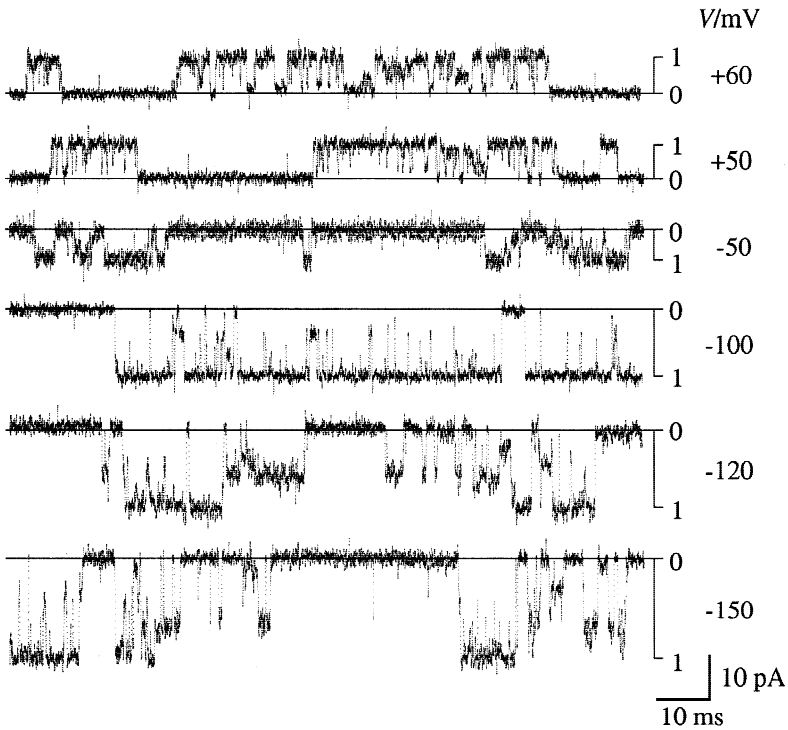

Fig. 5. Single channel current recordings in polyconductance state at various voltages as indicated; 0: baselines; 1: mean currents at full conductance; conditions: cytoplasmic 250 mM K^+, 20 mM Na^+, and 0.1 mM Ca^{2+}; luminal 150 mM K^+, 1 mM Ca^{2+}; original data filtered with 3 kHz (Gaussian) for illustration purpose.

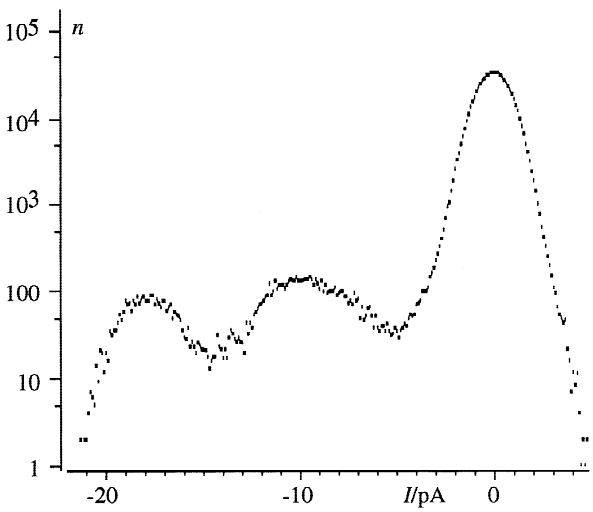

Fig. 6. Current-data accumulations during a 16.5 sec time series (V = −120 mV) from experiment Fig. 5; selective amplitude histogram according to Patlak (1988) with exclusion criterion 6.5 pA (= SD of background noise), 100 μsec time window (20 data points), and 50 kHz effective filtering.

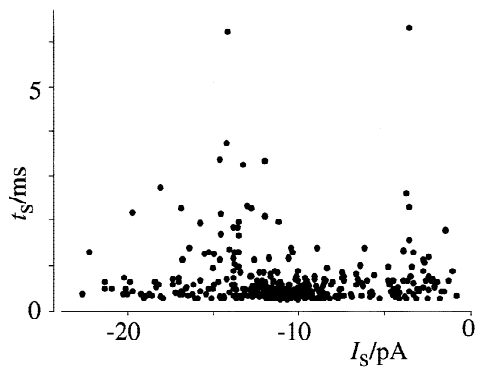

Fig. 7. Durations t_s of subconductance currents I_s (at −150 mV) in polyconductance state; temporal resolution 290 μsec (36 data points): time intervals in which σ of the currents is not significantly different from σ of baseline; I_s: mean currents during time intervals t_s; about 300 intervals t_s identified; full open channel currents (−22 pA) not displayed.

differences (e.g., requirement of Na^+ and number of subconductance levels) between the midstate (Tyerman et al., 1992) and the polysubconductance mode presented here are typical for $Ch_{T,K}$ as it shows up in numerous characteristic modes.

We suggest that the polyconductance mode is a Na^+-induced state of $Ch_{T,K}$ in which not only the main gate(s) and selectivity filter determine the throughput of charges at a given driving force but that many of the possible conformations of the pore protein can contribute as well to the rate limitation of the channel.

This work has been supported by the Deutsche Forschungsgemeinschaft. We thank Drs. Ulrike Homann and Gerhard Thiel for critical reading of the manuscript, and Dr. Adam Bertl for valuable discussions.

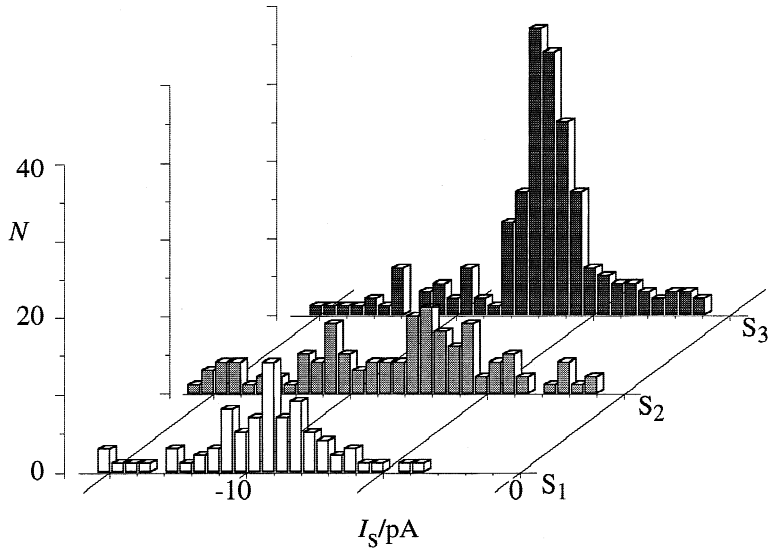

Fig. 8. Histograms of mean current amplitude levels (at −120 mV) in polyconductance state, separated in classes S_1: transitions from baseline to intermediate current levels and back, S_3: transitions from full open channel current (−18 pA) to intermediate levels and back, S_2: all other transitions.

References

Bertl, A. 1989. Current-voltage relationships of a sodium-sensitive potassium channel in the tonoplast of *Chara corallina. J. Membrane Biol.* **109:**9–19

Bertl, A. et al. 1992. Electrical measurements on endomembranes. *Science* **258:**873–874

Draber, S., Hansen, U.P. 1994. Fast single-channel measurements resolve the blocking effect of Cs^+ on the K^+ channel. *Biophys. J.* **67:**120–129

Draber, S., Schultze, R. 1994. Correction for missed evens based on a realistic model of a detector. *Biophys. J.* **66:**191–201

FitzHugh, R. 1983. Statistical properties of the asymmetric random telegraph signal, with applications to single-channel analysis. *Math. Biosci.* **64:**76–89

Hansen, U.P., Keunecke, M., Blunk, R. 1997. Gating and permeation models of plant channels. *J. Exp. Bot.* **48:**365–382

Klieber, H.G., Gradmann, D. 1993. Enzyme kinetics of the prime K^+ channel in the tonoplast of *Chara:* selectivity and inhibition. *J. Membrane Biol.* **132:**253–265

Laver, D.R., Walker, N.A. 1987. Steady-state voltage-dependent gating and conduction of the K^+ channel in the membrane of cytoplasmic drops from *Chara australis. J. Membrane Biol.* **100:**31–42

Laver, D.R., Cherry, C.A., Walker, N.A. 1997. The actions of calmodulin antagonists W-7 and TFP and of calcium on the gating kinetics of the calcium-activated large conductance potassium channel of the *Chara* protoplasmic drop: a substate-sensitive analysis. *J. Membrane Biol.* **155:**263–74

Laver, D.R., Gage, P.W. 1997. Interpretation of substates in ion channels: unipores or multipores? *Prog. Biophys. Mol. Biol.* **67:**99–140

Lühring, H. 1999. pH-sensitive gating kinetics of the maxi-K channel in the tonoplast of *Chara australis. J. Membrane Biol.* **168:**47–61

Penner, R. 1995. A practical guide to patch clamping. *In:* Single-Channel Recording, B. Sakmann and E. Neher, editors, pp. 3–30. Plenum Press, New York

Tyerman, S.D., Terry, B.R., Findlay, G.P. 1992. Multiple conductances in the large K^+ channel from *Chara corallina* shown by a transient analysis method. *Biophys. J.* **61:**726–749